# Design of Hybrid Wireless and Power Line Sensor Networks With Dual-Interface Relay in IoT

Yuwen Qian, Jiahui Yan, Haibing Guan, Jun Li, *Senior Member, IEEE*, Xiangwei Zhou, *Senior Member, IEEE*, Shengjie Guo, and Dushantha Nalin K. Jayakody, *Member, IEEE*

***Abstract*—The hybrid wireless and power line communication (HWPLC) networks address the problem that mobile wireless sensors and power line communication (PLC) sensors cannot communicate with each other within an Internet of Things (IoT) network. In this paper, we design a relay equipped with a dual wireless and PLC interface, which connects both the PLC and wireless sensors into an IoT network. Furthermore, the dual-interface relay forwards messages by adaptively selecting a interface according to the channel state. A general mathematical probability model of the dual-interface relaying system is presented. The probability density function of the output signal-to-noise ratio (SNR) is developed, which is based on explicit closed-form expressions derived from the statistics character of the PLC and wireless channel. Furthermore, the average capacity, bit-error rate (BER) expressions, and the outage probability formulas are derived. Numerical results show that the HPLWC relaying system with the dual-interface can significantly improve the performance of capacity, BER, and outage probability by adaptively selecting the interface with the optimal received SNR.**

***Index Terms*—Capacity, Internet of Things (IoT), outage probability, power line communications (PLCs), sensor networks, wireless networks.**

## I. Introduction

THE INTERNET of Things (IoT) is treated as the promising digital communication system with a wide range of applications, such as sensors, smart devices, smart metering, and control systems [1]. Communication is the bridge to bond all the sensors, actuators, management systems, and databases together to form the IoT. Traditionally, wireless communications are considered as the key to provide connectivity for the IoT. However, with the rapid development of the smart grid system, the important and fruitful area in IoT, power line communication (PLC) has become a competitive candidate communication technology for IoT systems, due to its advantages such as easy-to-use, cost efficiency, and simple installations [2].

However, using wireless communication and PLC is challenging in an IoT network. On one hand, due to the physical connections between the PLC transceivers and the electrical power grid, it is difficult for mobile users to connect to a PLC network [3]. On the other hand, wireless communications is not preferable for the smart home networks because many intelligent appliances and sensors, such as energy consumption monitors and multimedia devices, require connections to the household alternating current (ac) power distribution network for practical implementation [4]. In this scenario, according to [5], a hybrid wireless and PLC (HWPLC) network is an effective solution for IoT systems, where heterogeneous sensors can access.

Many recent efforts have been applied to conceive both PLC and wireless communication technologies in the IoT. To offer mobility to PLC users and to provide ac interfaces to household mobile devices, solutions encompassing both PLC and wireless transceivers have been introduced to IoT systems [6], [7]. In HWPLC networks, the combination of PLC and wireless communications improves the throughput, stability, and quality of service [8]. Inspired by this idea, several hardware and software products with HWPLC interfaces are developed for the IoT networks in the various scenarios [9]. Besides the standard, IEEE 1905.1 is produced to define the network enabler for supporting both wireless and PLC technologies [10].

However, both PLC and wireless communications suffer severe signal attenuation in long distance transmissions [11], [12]. Therefore, long distance information transmission is a challenge in HWPLC networks. To overcome long distance transmission in HWPLC networks, many researches focus on enhancing reliability and extending transmission range. Since the relaying scheme provides robustness and fast communication, the relay aided network becomes an attractive option.

Manuscript received March 11, 2017; revised June 20, 2017; accepted July 5, 2017. Date of publication July 11, 2017; date of current version February 25, 2019. This work was supported in part by the National Natural Science Foundation of China under Grant 61501238, in part by the Jiangsu Provincial Science Foundation under Project BK20150786, in part by the Specially Appointed Professor Program in Jiangsu Province 2015, in part by the Fundamental Research Funds for the Central Universities under Grant 30916011205, in part by the Open Research Fund of National Mobile Communications Research Laboratory, Southeast University, under Grant 2017D04, and in part by the Ningbo Natural Science Fund Project under Grant 2016A610110. *(Corresponding author: Jun Li.)*

Y. Qian and J. Yan are with the School of Electronic and Optical Engineering, Nanjing University of Science and Technology, Nanjing 210094, China (e-mail: admon@njust.edu.cn; jiahui@njust.edu.cn).

H. Guan is with the Department of Computer Science and Engineering, School of Electronic, Information and Electronic Engineering, Shanghai Jiao Tong University, Shanghai 200240, China (e-mail: hbguan@sjtu.edu.cn).

J. Li is with the School of Electronic and Optical Engineering, Nanjing University of Science and Technology, Nanjing 210094, China, and also with the National Mobile Communications Research Laboratory, Southeast University, Nanjing 210018, China (e-mail: jun.li@njust.edu.cn).

X. Zhou and S. Guo are with the Division of Electrical and Computer Engineering, Louisiana State University, Baton Rouge, LA 70803 USA (e-mail: xwzhou@lsu.edu; sguo12@lsu.edu).

D. N. K. Jayakody is with the Department of Software Engineering, Institute of Cybernetics, National Research Tomsk Polytechnic University, Tomsk 634034, Russia (e-mail: nalin@tpu.ru).

Digital Object Identifier 10.1109/JIOT.2017.2725451

Relay is originally emerged as a promising way to improve performance of wireless networks, which has been extensively studied. Through installing relays, wireless networks extend transmission range and improve transmission reliability. The relaying idea has been adopted recently to design relaying PLC networks [13], [14]. Nevertheless, channel characteristics of the PLC channel and wireless channel are quite different [12], [15]. The wireless relaying techniques cannot be adopted directly in PLC networks. Thus, a TDMA-based relay-aided PLC scheme for a network management system has been studied in [16]. Lampe *et al.* [17] have extended the transmission in PLC relaying networks. Lai and Messier [4] investigated the cooperative relaying protocol in a PLC In-Home network and analyzes the performance with a statistical topology model.

Moreover, recent researches focus on cooperative PLC relaying system in HWPLC networks [18]–[20]. A cooperative relaying communication approach based on fountain codes has been introduced to lessen the fading impacts in narrowband PLC channel [18]. The cooperative relay over multiple-input multiple-output (MIMO) channel has been devised for HWPLC network in [19], where the capacity of the MIMO channel is analyzed. However, the capacity is derived based on a special physical model. Kuhn *et al.* [20] have proposed to use the relaying scheme to combine wireless LANs and PLC networks, which improves the robustness of the hybrid networks. However, since HWPLC relaying scheme is an emerging topic, no comprehensive analyses have yet been conducted.

Therefore, in this paper, we focus on designing an HWPLC relaying sensor network for IoT system and analyzing the end-to-end performance for this system. Various performance measures of relaying HWPLC systems have been studied. In particular, we list fourfold contributions of this paper as following.

1) A dual-interface relaying scheme to combine the power line and wireless communication is proposed for sensor networks in IoT systems. The cooperative communication mechanism is implemented at the relaying node equipped with dual-interface, where interface with optimal channel can be specialized to forward information.
2) We model the PLC channel by combining several PLC subchannels, which suffer the lognormal fading and impulsive noise. Then the distribution of the received signal-to-noise ratio (SNR) for PLC channels has been formulated as a lognormal sum function.
3) We adopt an accurate mathematical approximation for the lognormal sum function to derive the probability density function (PDF) and the cumulative distribution function (CDF) of the received SNR for PLC channels. The incomplete gamma function is used to develop the closed-form of CDF of the received SNR for wireless channels.
4) By employing the derived CDF of SNR in the PLC and wireless channels, we develop the closed-form of the average capacity and bit-error rate (BER), based on Tayor's extending and Hermite polynomial. By resorting to the Bayesian probability, we derive the closed-form of outage probability.
5) In simulation, numerical results demonstrate that the derived analytical results are consistent with that of Monte-Carlo simulations, and the performance of the proposed hybrid relaying scheme outperforms the single communication scheme of either the wireless relay or the PLC relay.

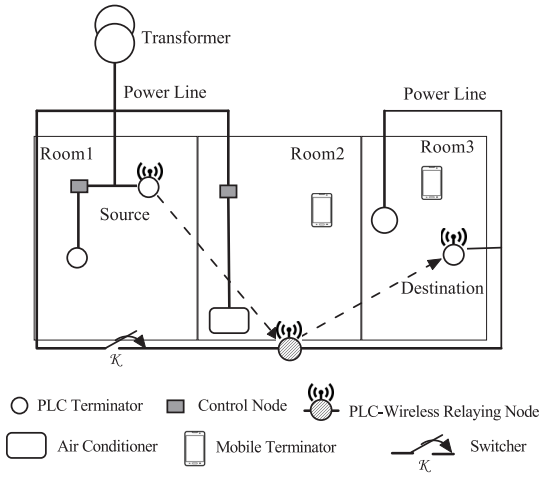


Fig. 1. Structure of a typical IoT system with relaying nodes, which have a PLC interface and wireless interface. Wireless and PLC sensors are distributed in various rooms and PLC sensors are installed in electrical loads and connected by the power line cables.

The rest of this paper is organized as follows. Section II introduces the system model. Section III presents the statistics of the SNR of two links of the relay with PLC and wireless interfaces. In Section IV, various end-to-end performance analyses of HWPLC relaying networks are evaluated. Finally, in Section V, the conclusions are drawn.

## II. System Model

In this paper, we consider a typical IoT system, equipped with both wireless and PLC sensors, where PLC sensors are installed in the electrical loads and meters. Since sensors can perform as routes or terminal nodes, the proposed sensor network forms as an ad hoc, as shown in Fig. 1.

In particular, PLC is instable via lengthened power line between sensors and so does wireless communication when there exist several walls between the transceivers. To cope with this instability, the dual-interface relaying nodes, which have a PLC and wireless interface, are installed. Generally, the dual-interface relaying nodes are installed at some selected, crucial points of the network. For example, in Fig. 1, room 1 and room 3 are independent ad hoc which cannot directly communicate due to the long distance between the two rooms. In this scenario, a relay with PLC-wireless interface is deployed to aid communications for sensors in the two networks. Since we cannot equip all sensors with this dual-interface due to high investment and energy cost. Only a few nodes near the dual-interface relaying node are installed with the dual-interface. Therefore, both mobile terminals and fixed PLC sensors can conveniently access to the network. Furthermore,

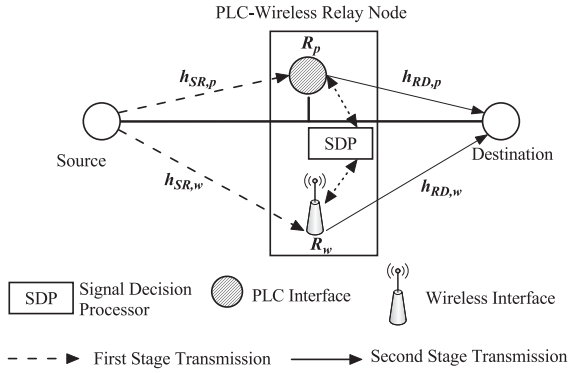


Fig. 2. Logical structure of a typical HWPLC relaying scheme with two-stage relay transmitting protocol, $R_p$ and $R_w$ are the PLC and wireless interface, the SDP is the signal decision processor, which can select the signal with higher SNR from the two interfaces, $h_{\mathrm{SR},p}$ and $h_{\mathrm{SR},w}$ are the channel gains from $\mathcal{S}$ to $\mathcal{R}$ via PLC and wireless channels, and $h_{\mathrm{RD},p}$ and $h_{\mathrm{RD},w}$ are the PLC and wireless channel gains from $\mathcal{R}$ to $\mathcal{D}$.

this dual-interface relaying scheme provides robust communication for the sensor networks, since if one of the two communications is out of work, the other can be used to maintain the network connection.

In relaying system in Fig. 1, a source node $\mathcal{S}$ in room 1 communicates with the destination terminal $\mathcal{D}$ via the relaying node $\mathcal{R}$, which works in the half-duplex mode. The transmission from $\mathcal{S}$ to $\mathcal{D}$ includes two hops, which is illustrated in Fig. 2.

In Fig. 2, there are two stages during the transmission and each has one time slot. In the first time slot, $\mathcal{S}$ broadcasts the message over the wireless and PLC channels to the relaying node. The received signals at the relaying node can be written as

$$\begin{bmatrix} y_{\mathrm{SR},p}(t) \\ y_{\mathrm{SR},w}(t) \end{bmatrix} = \begin{bmatrix} \sqrt{P_S} & 0 \\ 0 & \sqrt{P_S} \end{bmatrix} \begin{bmatrix} h_{\mathrm{SR},p} & 0 \\ 0 & h_{\mathrm{SR},w} \end{bmatrix} \begin{bmatrix} x(t) \\ x(t) \end{bmatrix} + \begin{bmatrix} n_{\mathrm{SR},p}(t) \\ n_{\mathrm{SR},w}(t) \end{bmatrix} \tag{1}$$

where $x(t)$ is the transmitted symbol, $h_{\mathrm{SR},p}$ and $h_{\mathrm{SR},w}$ are the channel gains from $\mathcal{S}$ to $\mathcal{R}$ over PLC and wireless channels, respectively, the subscripts $p$ and $w$ stand for the PLC and wireless channels, respectively, $P_S$ is the transmission power, and $n_{\mathrm{SR},p}(t)$ and $n_{\mathrm{SR},w}(t)$ are the noise over the PLC channel and wireless channel, respectively.

To achieve better performance, a signal decision processor (SDP) module in the relaying node selects the interface with the higher received SNR to forward the received information. In each time block, the PLC and wireless interfaces receive the message via their communication channels and then the received SNRs can be calculated, which are imputed to the SDP. According to the two input SNRs, SDP module selects an optimal relaying channel from the wireless and PLC channels. Therefore, the received SNR at the relaying node can be expressed as

$$\gamma_{\mathrm{SR}} = \max\left\{P_S h_{\mathrm{SR},p}^2/{\sigma_p}^2, P_S h_{\mathrm{SR},w}^2/{\sigma_w}^2\right\} \tag{2}$$

where ${\sigma_p}^2$ is the variance of the noise over the PLC channel and ${\sigma_w}^2$ is the variance of the noise over wireless channel.

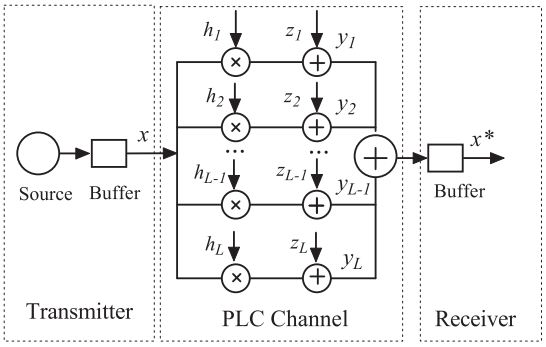


Fig. 3. Structure of a diversity PLC channel with $L$ subchannels, $x$ and $x^*$ are the input and output signals of the PLC channel, $h_l$ $(1 \le l \le L)$ is the channel gain of the $l$th PLC subchannel, $z_l$ $(1 \le l \le L)$ is noise of the $l$th PLC subchannel, and $y_l$ $(1 \le l \le L)$ is output signal of the $l$th PLC subchannel.

In the second time slot, the received signals at destination can be written as

$$\begin{bmatrix} y_{\mathrm{RD},p}(t) \\ y_{\mathrm{RD},w}(t) \end{bmatrix} = \begin{bmatrix} \sqrt{P_R} & 0 \\ 0 & \sqrt{P_R} \end{bmatrix} \begin{bmatrix} h_{\mathrm{RD},p} & 0 \\ 0 & h_{\mathrm{RD},w} \end{bmatrix} \begin{bmatrix} y_{\mathrm{SR}}(t) \\ y_{\mathrm{SR}}(t) \end{bmatrix} + \begin{bmatrix} n_{\mathrm{RD},p}(t) \\ n_{\mathrm{RD},w}(t) \end{bmatrix} \tag{3}$$

where $y_{\mathrm{SR}}(t)$ is the selected signal at the relaying node, $h_{\mathrm{RD},p}$ and $h_{\mathrm{RD},w}$ are the channel gains from $\mathcal{R}$ to $\mathcal{D}$ over the PLC channel and wireless channel, respectively, $P_R$ is the transmission power of the relaying node, and $n_{\mathrm{RD},p}(t)$ and $n_{\mathrm{RD},w}(t)$ are the noise over the PLC and wireless channels, respectively.

Moreover, at the terminal $\mathcal{D}$, the interface with higher received SNR is selected to receive data. The received SNR at $\mathcal{D}$ is formulated as

$$\gamma_{\mathrm{RD}} = \max\left\{P_R h_{\mathrm{RD},w}^2/{\sigma_p}^2, P_R h_{\mathrm{RD},w}^2/{\sigma_w}^2\right\}. \tag{4}$$

In our model, we assume that $\mathcal{S}$ and $\mathcal{R}$ transmit symbols with unit power, that $P_S = P_R = 1$.

## III. Statistical Analysis for HWPLC Channels

In this section, we consider the PLC systems with the multiple branches diversity combining receiver, as shown in Fig. 3. There is buffer installed at the PLC transmitter to collect and store data from the source node. The transmitter then transmits the stored data as binary phase shift keying (BPSK) modulated symbols over $L$ correlated PLC subchannels, which can be combined from frequency, time, and space. Each of these subchannels has multiple subfrequency bands with sufficient separation to avoid cross channel interference. We assume that the receiver is well synchronised with the transmitter. In addition, there is a buffer equipped at the receiver to store received symbols. By using the MRC scheme, the receiver can combine the correlated received signals from the $L$ PLC subchannels.

The received signal at the receiving node from the $l$th, $(1 \le l \le L)$, PLC subchannel is [12]

$$y_l = h_l x_l + z_l, \quad 1 \le l \le L \tag{5}$$

where $x_l$ is the transmitted signal over the $l$th subchannel, $h_l$ is the channel gain of the $l$th subchannel, and $z_l$ is the received noise over the $l$th subchannel.

According to [12], since a PLC subchannel is subject to the mixture of the thermal and impulsive noises that are independent, the Bernoulli–Gaussian model can be adopted as the noise model for PLC channels, which is

$$z_l = n_G + n_B \times n_I \tag{6}$$

where $n_G$ and $n_I$ are Gaussian random variables with zero mean and variances $\sigma_G^2$ and $\sigma_I^2$, respectively, and $n_B$ is a Bernoulli random sequence with parameter $p$.

The variance of the PLC channel noise $\sigma_{p,l}$ can be further formulated as

$$\sigma_{p,l}^2 = E\left(n_G^2\right) + E\left(n_B^2\right) \times E\left(n_I^2\right) = \sigma_G^2 + p\sigma_I^2. \tag{7}$$

Since $L$ subchannels are assumed interference-free with each other, the noises in subchannels are independent and identical. Thus, we have $\sigma_p = \sigma_{p,1} = \cdots = \sigma_{p,L}$.

As in [12] and [21], the PDF of $h_l$ is lognormal, expressed as

$$f_{h_l}(x) = \frac{1}{\sqrt{2\pi\sigma^2}x} e^{-\frac{(\ln x-\mu)^2}{2\sigma^2}} \tag{8}$$

where $\mu$ and $\sigma^2$ are the mean and the variance of a normal random variable $\ln(h_l)$, respectively.

As shown in Fig. 3, the input signals are transmitted via different subchannels from $\mathcal{S}$ to $\mathcal{D}$. The MRC is adopted to obtain the optimal received SNR over the PLC channel [22], which is

$$\gamma_{\mathrm{SR},p} = \frac{\left(\sum_{l=1}^{L} w_l h_l\right)^2}{\sum_{l=1}^{L} w_l^2 \sigma_{p,l}^2} = \frac{1}{\sigma_{p,l}^2} \frac{\left(\sum_{l=1}^{L} w_l h_l\right)^2}{\sum_{l=1}^{L} w_l^2} \tag{9}$$

where $w_l$ is the weight over the $l$th subchannel, $\gamma_{\mathrm{SR},p}$ is the received SNR of the link from $\mathcal{S}$ to $\mathcal{R}$ over PLC channels.

Since $w_l$ is proportional to the channel gain in MRC, without loss of generality, we define $w_l = c \times h_l$, where $c$ is a constant. The received SNR is thereby rewritten as

$$\gamma_{\mathrm{SR},p} = \frac{1}{\sigma_{p,l}^2} \frac{c^2\left(\sum_{l=1}^{L} h_l^2\right)^2}{c^2 \sum_{l=1}^{L} h_l^2} = \sum_{l=1}^{L} \frac{h_l^2}{\sigma_{p,l}^2}. \tag{10}$$

Furthermore, the received SNR can be denoted as

$$\gamma_{\mathrm{SR},p} = \gamma_p \sum_{l=1}^{L} h_l^2 \tag{11}$$

where the transmit SNR over the $l$th PLC subchannel $\gamma_p \triangleq (1/\sigma_p^2)$.

With the character of the lognormal function, $h_l^2$ follows the lognormal distribution with mean $2\mu$ and vairance $\sigma^2$. Define $\mu_\gamma = 2\mu$ and $\sigma_\gamma = \sigma$. We then have the PDF of $h_l^2$ as

$$f_{h_l^2}(x) = \frac{1}{\sqrt{2\pi\sigma_\gamma^2}x} e^{-\frac{\left(\ln x-\mu_\gamma\right)^2}{2\sigma_\gamma^2}}. \tag{12}$$

According to (11), the received SNR of the PLC channel follows lognormal sum distribution. Therefore, the derivation of the CDF of SNR for PLC channels needs to solve an integral of the lognormal sum, which is a great challenge. In this scenario, we approximate the PDF of $\gamma_{\mathrm{SR},p}$ as [23]

$$f_{\gamma_{\mathrm{SR},p}}(x) \approx \frac{a_1 a_2 \left(\frac{x}{\gamma_p}\right)^{-(a_2/\lambda+1)}}{\sqrt{2\pi}\lambda\gamma_p} \times \exp\left(-\frac{\left(a_0 - a_1\left(\frac{x}{\gamma_p}\right)^{-a_2/\lambda}\right)^2}{2}\right) \tag{13}$$

where $\lambda = (\ln 10/10)$ and $a_0$, $a_1$, and $a_2$ are constants.

Based on (13), the CDF of $\gamma_{\mathrm{SR},p}$ is obtained as

$$F_{\gamma_{\mathrm{SR},p}}(x) = \Phi\left(a_0 - a_1\left(\frac{x}{\gamma_p}\right)^{-a_2/\lambda}\right) \tag{14}$$

where $\Phi(x) = \int_0^x (1/\sqrt{2\pi}) e^{-(t^2/2)} \mathrm{d}t$ is the Gaussian function with zero mean and unity variance.

Since the two stages of the relaying scheme are independent, we can obtain the same CDF and PDF of $\gamma_{\mathrm{RD},p}$, which are $f_{\gamma_{\mathrm{RD},p}} \approx f_{\gamma_{\mathrm{SR},p}}$ and $F_{\gamma_{\mathrm{RD},p}} \approx F_{\gamma_{\mathrm{SR},p}}$, where $f_{\gamma_{\mathrm{SR},p}}$ and $F_{\gamma_{\mathrm{RD},p}}$ are the PDF and CDF of the received SNR at $\mathcal{D}$, respectively.

Then we consider the statistical characters of the wireless channel. In practical IoT networks, the Nakagami-$m$ model is generally adopted as the distribution for the wireless channel gain $h_w$, whose PDF is given by

$$f_{h_w}(x) = \frac{2m^m x^{2m-1}}{\Gamma(m)\Omega^m} \exp\left(-\frac{m}{\Omega}x^2\right) \tag{15}$$

where $m = [\mathbb{E}^2(x^2)/\sigma(x^2)]$, $\Omega = \mathbb{E}(x^2)$, $\Gamma(x) = \int_0^\infty t^{x-1}e^{-t}\mathrm{d}t$, and $\mathbb{E}(\cdot)$ is the statistical expectation operator.

Define the transmit SNR for the wireless channel $\gamma_w \triangleq (1/\sigma_w^2)$ and we have $\gamma_{\mathrm{SR},w} = \gamma_w h_w^2$. According to (15), we can derive the PDF of the received SNR at the relay for wireless channel as

$$f_{\gamma_{\mathrm{SR},w}}(x) = \frac{\left(\frac{m}{\gamma_w\Omega}\right)^m x^{m-1}}{\Gamma(m)} \exp\left(-\frac{m}{\gamma_w\Omega}x\right). \tag{16}$$

In addition, it follows that [24]:

$$\int_0^u x^{v-1}e^{-\mu x}\mathrm{d}x = \mu^{-v}\Upsilon(v, \mu u) \tag{17}$$

where $\Upsilon(\alpha, x) = \sum_{n=0}^{\infty}[((-1)^n x^{\alpha+n})/(n!(\alpha+n))]$.

By combining (16) and (17), the CDF of the received SNR over the wireless channel is expressed as

$$F_{\gamma_{\mathrm{SR},w}}(x) = \frac{\left(\frac{m}{\gamma_w\Omega}\right)^m}{\Gamma(m)} \int_0^x t^{m-1}e^{-\frac{m}{\gamma_w\Omega}t}\mathrm{d}t = \frac{\Upsilon\left(m, \frac{m}{\gamma_w\Omega}x\right)}{\Gamma(m)}. \tag{18}$$

## IV. Performance Analysis

In this section, we analyze the performance of the average capacity, outage probability, and average BER for the HWPLC relaying system described in the previous section.

### A. Average Capacity

The average channel capacity is an important performance metric for communication channels, which reveals the maximum amount of information that can be transmitted. The average capacity of the relaying system is defined as

$$C_{av} = \min(C_{\mathrm{SR}}, C_{\mathrm{RD}}) \tag{19}$$

where $C_{\mathrm{SR}}$ is the capacity of the link from $\mathcal{S}$ to $\mathcal{R}$ and $C_{\mathrm{RD}}$ is the capacity of the link from $\mathcal{R}$ to $\mathcal{D}$.

Since the link from $\mathcal{S}$ to $\mathcal{R}$ is comprised of two parallel channels, the PLC and wireless channel, the capacity of the link is expressed as

$$C_{\mathrm{SR}} = C_{\mathrm{SR},p} + C_{\mathrm{SR},w} \tag{20}$$

where $C_{\mathrm{SR},p}$ and $C_{\mathrm{SR},w}$ are the capacities of the link from $\mathcal{S}$ to $\mathcal{R}$ over the PLC and wireless channels, respectively.

Similarly, we have

$$C_{\mathrm{RD}} = C_{\mathrm{RD},p} + C_{\mathrm{RD},w} \tag{21}$$

where $C_{\mathrm{RD},p}$ and $C_{\mathrm{RD},w}$ are the capacities of the link from $\mathcal{R}$ to $\mathcal{D}$ over the PLC and wireless channels, respectively.

*1) Capacity of the PLC Channel:* The PLC channel suffers the Bernoulli–Gaussian noise [25], which is considered as a two states Gaussian noise. The capacity of the PLC channel $C_p(\gamma)$ is given as [26], [27]

$$C_p(\gamma) = \sum_{j=0}^{1} p_j \log_2\left(1 + \gamma\alpha_j\right) \tag{22}$$

where $\gamma$ is the received SNR, $p_0 = 1-p$, $p_1 = p$, and $\alpha_0$ and $\alpha_1$ are given as

$$\alpha_0 = 1 + p\eta, \alpha_1 = \frac{1+p\eta}{1+\eta} \tag{23}$$

where $\eta \triangleq (\sigma_I^2/\sigma_G^2)$.

In a high SNR regime, we have $\gamma_0\alpha_0 \gg 1$ and $\gamma_0\alpha_1 \gg 1$. Thus, the capacity can be approximated as

$$C_p(\gamma) \approx \Theta(p) + \frac{\ln\gamma}{\ln 2} \tag{24}$$

where $\Theta(p) = (1-p)\log_2(\alpha_0) + p\log_2(\alpha_1)$ and the average capacity can be expressed as

$$C_{\mathrm{SR},p} = \int_0^\infty C_p(x)\mathrm{d}F_{\gamma_{\mathrm{SR},p}}(x). \tag{25}$$

With (14), (24), and (25), the average capacity of the PLC channel is given as

$$\begin{aligned} C_{\mathrm{SR},p} &= \int_0^\infty C_p(x)\mathrm{d}F_{\gamma_{\mathrm{SR},p}}(x) \\ &= \Theta(p) + \int_0^\infty \log_2(x)\mathrm{d}\Phi\left(a_0 - a_1\left(\frac{x}{\gamma_p}\right)^{-a_2/\lambda}\right). \end{aligned} \tag{26}$$

Let $s = a_0 - a_1((x/\gamma_p))^{-a_2/\lambda}$. Then we have

$$\begin{aligned} C_{\mathrm{SR},p} = \Theta(p) + \frac{1}{\sqrt{2\pi}}\int_{-\infty}^{\infty}\left(\log_2\gamma_p + \frac{\lambda}{a_2}\log_2\left(\frac{a_1}{a_0-s}\right)\right) \\ \times\ e^{-\frac{s^2}{2}}\mathrm{d}s. \end{aligned} \tag{27}$$

According to [28], the following approximation holds:

$$\int_{-\infty}^{\infty} f(x)e^{-x^2}\mathrm{d}x \approx \sum_{i=1}^{N} w_i f(x_i) \tag{28}$$

where $N$ is the order of the Hermite polynomial, $w_i = [2^{n-1}n!\sqrt{\pi}/n^2(H_{n-1}(x_i))^2]$ is the $i$th weight, and $x_i$ is the $i$th zero of the Hermite polynomial $H_n(x)$.

Substituting (28) in (27), the average capacity of the PLC channel is obtained as

$$\begin{aligned} C_{\mathrm{SR},p} = \Theta(p) + \frac{1}{\ln 2\sqrt{\pi}}\sum_{i=1}^{N} w_i \\ \times\ \left(\ln\gamma_p + \frac{\lambda}{a_2}\ln\left(\frac{a_1}{a_0 - \sqrt{2}q_i}\right)\right). \end{aligned} \tag{29}$$

*2) Capacity of the Wireless Channel:* Since the noise of wireless channels is Gaussian noise, the capacity of a wireless channel can be written as

$$C_w(\gamma) = \log_2(1+\gamma). \tag{30}$$

According to (30), the average capacity for the wireless channel of the link from $\mathcal{S}$ to $\mathcal{R}$ is given as

$$\begin{aligned} C_{\mathrm{SR},w} = \int_0^\infty \log_2(1+x)\frac{\left(\frac{m}{\gamma_w\Omega}\right)^m x^{m-1}}{\Gamma(m)} \\ \times\ \exp\left(-\frac{m}{\gamma_w\Omega}x\right)\mathrm{d}x. \end{aligned} \tag{31}$$

Define $x = (\gamma_w\Omega q^2/m)$. The average capacity of the wireless channel is rewritten as

$$\begin{aligned} C_{\mathrm{SR},w} &= \frac{2}{\ln 2\Gamma(m)}\int_{-\infty}^{\infty}\left(\ln\left(\gamma_w\Omega q^2\right) - \ln m\right)q^{2m-1}\mathrm{e}^{-q^2}\mathrm{d}q \\ &= \frac{2}{\ln 2\Gamma(m)}\sum_{i=1}^{N} w_i\left(\ln\left(\gamma_w\Omega q_i^2\right) - \ln m\right)q_i^{2m-1}. \end{aligned} \tag{32}$$

Since the links of the first hop and the second hop are identical and work independently in different time slots, we have $C_{\mathrm{SR},w} \approx C_{\mathrm{RD},w}$ and $C_{\mathrm{SR},p} \approx C_{\mathrm{RD},p}$. According to (19)–(21), the average capacity of the relaying system with dual-interface can be given as (33), shown at the bottom of the next page.

### B. Outage Probability

In the HWPLC relaying system as shown in Fig. 1, we define $O_t$ to represent the outage events, where $t$ is an indicator that $t = \mathrm{SR}$ is the outage events in the first stage and $t = \mathrm{RD}$ denotes the outage events in the second stage. As outage events occur either in the first or the second stage or both, the transmission is outage.

Accordingly, the outage event is defined as

$$O_t \triangleq \bigcup_{\mathcal{A}} O_{t,\mathcal{A}} \tag{34}$$

where $\mathcal{A}$ denotes the wireless or PLC channel. If $\mathcal{A} = w$, $O_{t,\mathcal{A}}$ means the outage events set occurring in the wireless channel. If $\mathcal{A} = p$, $O_{t,\mathcal{A}}$ represents the outage events set occurring in the PLC channel.

Since the outage probability is defined as the probability that the transmission rate $T$ is greater than the channel mutual information, the outage probability $O_{t,A}$ is expressed as

$$O_{t,\mathcal{A}} \triangleq \left\{ I(x_{\mathcal{A}}; y_t | x_{\mathcal{A}}) = I_{t,\mathcal{A}} \leq T_{t,\mathcal{A}} \right\} \tag{35}$$

where $T_{t,\mathcal{A}}$ is the capacity of the $t$ time slot and $\mathcal{A}$ channel, and $I$ is the mutual information.

The outage probability of the HWPLC relaying system is given as

$$P_o(O) = P_o(O_{\mathrm{SR}}) + P_o(O_{\mathrm{RD}}) - P_o(O_{\mathrm{SR}}) P_o(O_{\mathrm{RD}}) \tag{36}$$

where $P_o(O_{SR})$ is the outage probability of the link from $\mathcal{S}$ to $\mathcal{R}$, which is

$$P_o(O_{\mathrm{SR}}) = P_o\big(O_{\mathrm{SR},p}\big) P_o\big(O_{\mathrm{SR},w}\big) \tag{37}$$

and $P_o(O_{\mathrm{RD}})$ is the outage probability of the link from $\mathcal{R}$ to $\mathcal{D}$, which is

$$P_o(O_{RD}) = P_o\big(O_{\mathrm{RD},p}\big) P_o\big(O_{\mathrm{RD},w}\big) \tag{38}$$

where $P_o(O_{\mathrm{SR},p})$ and $P_o(O_{\mathrm{RD},p})$ are the outage probabilities of the PLC channels of the link from $\mathcal{S}$ to $\mathcal{R}$ and from $\mathcal{R}$ to $\mathcal{D}$, respectively, and $P_o(O_{\mathrm{SR},w})$ and $P_o(O_{\mathrm{RD},w})$ are the outage probabilities of the wireless channels of the link from $\mathcal{S}$ to $\mathcal{R}$ and from $\mathcal{R}$ to $\mathcal{D}$, respectively.

According to (35), the average outage probability can be expressed as

$$\begin{aligned} P_o\big(O_{\mathrm{SR},p}\big) &= P_o\big(I_{\mathrm{SR},p} \leq T_p\big) \\ &= P_o\left( \sum_{j=0}^{1} p_j \log_2\big(1 + \gamma_{\mathrm{SR},p} \alpha_j\big) \leq T_p \right). \end{aligned} \tag{39}$$

Combining (14) and (39), we have

$$\begin{aligned} P_o\big(O_{\mathrm{SR},p}\big) &\simeq F_{\gamma_{\mathrm{SR},p}}\big(2^{T_p} \alpha_0{}^{-p_0} \alpha_1{}^{-p_1}\big) \\ &= \Phi\left( a_0 - a_1 \left( \frac{2^{T_p} \alpha_0{}^{-p_0} \alpha_1{}^{-p_1}}{\gamma_p} \right)^{-a_2/\lambda} \right). \end{aligned} \tag{40}$$

Similarly, we can obtain the outage probability for the wireless channel as

$$\begin{aligned} P_o\big(O_{\mathrm{SR},w}\big) &= P_o\big(I_{\mathrm{SR},w} \leq T_w\big) \\ &= F_{\gamma_{\mathrm{SR},w}}\big(2^{T_w} - 1\big) \\ &= \frac{\Upsilon\left(m, \frac{m(2^{T_w}-1)}{\gamma_w \Omega}\right)}{\Gamma(m)}. \end{aligned} \tag{41}$$

According to (37), we have

$$\begin{aligned} P_o(O_{\mathrm{SR}}) &= P_o\big(O_{\mathrm{SR},p}\big) P_o\big(O_{\mathrm{SR},w}\big) \\ &= \Phi\left( a_0 - a_1 \left( \frac{2^{T_p} \alpha_0{}^{-p_0} \alpha_1{}^{-p_1}}{\gamma_p} \right)^{-a_2/\lambda} \right) \\ &\quad \times \frac{\Upsilon\left(m, \frac{m(2^{T_w}-1)}{\gamma_w \Omega}\right)}{\Gamma(m)}. \end{aligned} \tag{42}$$

Substituting (42) into (36), we obtain the closed-form of outage probability given in (43), shown at the bottom of this page.

### C. Average BER

In the dual-interface relaying system, the average BER depends on both two stages. However, as one signal is wrongly decoded in both the two links, the signal can be correctly received due to adopting the BPSK modulation. Therefore, the average BER of the entire relaying system can be expressed as

$$B = B_{\mathrm{SR}} + B_{\mathrm{RD}} - B_{\mathrm{SR}} \times B_{\mathrm{RD}} \tag{44}$$

where $B_{\mathrm{SR}}$ is the BER of the link from $\mathcal{S}$ to $\mathcal{R}$ and $B_{\mathrm{RD}}$ is the BER of the link from $\mathcal{R}$ to $\mathcal{D}$.

According to (2) and (4), the received message from the channel with higher received SNR is selected to be forwarded. Hence, the average BER is dominated by the channel which has a higher SNR. The average BER $B_{\mathrm{SR}}$ of the link from $\mathcal{S}$ to $\mathcal{R}$ can be given by

$$B_{\mathrm{SR}} = \min\big(B_{\mathrm{SR},p},\ B_{\mathrm{SR},w}\big) \tag{45}$$

where $B_{\mathrm{SR},p}$ is the average BER of the PLC channel of the link from $\mathcal{S}$ to $\mathcal{R}$ and $B_{\mathrm{SR},w}$ is the average BER of the wireless channel of the link from $\mathcal{S}$ to $\mathcal{R}$.

Similarly, $B_{\mathrm{RD}}$ can be expressed as

$$B_{\mathrm{RD}} = \min\big(B_{\mathrm{RD},p},\ B_{\mathrm{RD},w}\big) \tag{46}$$

$$C_{av} = \Theta(p) + \frac{1}{\ln 2\sqrt{\pi}} \sum_{i=1}^{N} w_i \left( \ln \gamma_p + \frac{\lambda}{a_2} \ln\left( \frac{a_1}{a_0 - \sqrt{2} q_i} \right) \right) + \frac{2}{\ln 2 \Gamma(m)} \sum_{i=1}^{N} w_i \Big( \ln\Big( \Omega \gamma_w q_i^2 \Big) - \ln m \Big) q_i^{2m-1} \tag{33}$$

$$\begin{aligned} P_o(O) = 2\Phi\left( a_0 - a_1 \left( \frac{2^{T_p} \alpha_0{}^{-p_0} \alpha_1{}^{-p_1}}{\gamma_p} \right)^{-a_2/\lambda} \right) \frac{\Upsilon\left(m, \frac{m(2^{T_w}-1)}{\gamma_w \Omega}\right)}{\Gamma(m)} - \Phi^2\left( a_0 - a_1 \left( \frac{2^{T_p} \alpha_0{}^{-p_0} \alpha_1{}^{-p_1}}{\gamma_p} \right)^{-a_2/\lambda} \right) \\ \times \frac{\Upsilon^2\left(m, \frac{m(2^{T_w}-1)}{\gamma_w \Omega}\right)}{\Gamma^2(m)} \end{aligned} \tag{43}$$

where $B_{\mathrm{RD},p}$ is the average BER of the PLC channel of the link from $\mathcal{R}$ to $\mathcal{D}$, and $B_{\mathrm{RD},w}$ is the average BER of the wireless channel of the link from $\mathcal{R}$ to $\mathcal{D}$.

With the assumption that the symbols transmitted by $\mathcal{S}$ and $\mathcal{R}$ have equal unit energies and equal priori probabilities, the conditional BER for the PLC channel conditioned on the SNR $\gamma$ can be expressed as [29]

$$B_p(\gamma) = \sum_{j=0}^{1} p_j Q\left(\sqrt{\alpha_j \gamma}\right) \tag{47}$$

where $Q(x) = (1/\sqrt{2\pi}) \int_x^\infty e^{-(t^2/2)} \mathrm{d}t$. Thus, average BER of the PLC channel $B_{\mathrm{SR},p}$ can be expressed as

$$\begin{aligned} B_{\mathrm{SR},p} &= \int_0^\infty B_p(\gamma) f_{\gamma_{\mathrm{SR},p}}(\gamma) \mathrm{d}\gamma \\ &= -\int_0^\infty B_p'(\gamma) F_{\gamma_{\mathrm{SR},p}}(\gamma) \mathrm{d}\gamma \end{aligned} \tag{48}$$

where $B_p'(\gamma)$ is the derivative of $B_p(\gamma)$ with respect to $\gamma$, which is

$$B_p'(\gamma) = -\sum_{j=0}^{1} \frac{p_j \sqrt{\alpha}_j}{2\sqrt{2\pi\gamma}} e^{-\frac{\alpha_j \gamma}{2}}. \tag{49}$$

Substituting (28) and (49) in (48), we obtain the BER of the PLC channel, written as

$$\begin{aligned} B_{\mathrm{SR},p} &= \int_0^\infty \sum_{j=0}^{1} \frac{p_j \sqrt{\alpha}_j}{2\sqrt{2\pi\gamma}} e^{-\frac{\alpha_j \gamma}{2}} F_{\gamma_{\mathrm{SR},p}}(\gamma) \mathrm{d}\gamma \\ &= \int_{-\infty}^\infty \sum_{j=0}^{1} \frac{p_j}{\sqrt{\pi}} e^{-q^2} F_{\gamma_{\mathrm{SR},p}}\left(\frac{2q^2}{\alpha_j}\right) \mathrm{d}q \\ &= \sum_{j=0}^{1} \sum_{i=1}^{N} w_i \frac{p_j}{\sqrt{\pi}} F_{\gamma_{\mathrm{SR},p}}\left(\frac{2q_i^2}{\alpha_j}\right) \\ &= \sum_{j=0}^{1} \sum_{i=1}^{N} w_i \frac{p_j}{\sqrt{\pi}} \Phi\left(a_0 - a_1 \left(\frac{2q_i^2}{\alpha_j \gamma_p}\right)^{-a_2/\lambda}\right). \end{aligned} \tag{50}$$

Similarly, the conditional BER of wireless channel is

$$B_w(\gamma) = aQ\left(\sqrt{\gamma b}\right) \tag{51}$$

where $a$, $b$ are constants, and $\gamma$ is the transmit SNR.

Substituting (18) in (51), we can obtain the BER of the wireless channel, given as

$$B_{\mathrm{SR},w} = \frac{a}{\sqrt{\pi}\Gamma(m)} \sum_{i=1}^{N} w_i \Upsilon\left(m, \frac{2mq_i^2}{\Omega b \gamma_w}\right). \tag{52}$$

Combining (50), (52), and (44), we obtain the average BER for the HWPLC relaying system given as (53), shown at the bottom of this page.

TABLE I
SIMULATION PARAMETERS SETTING

| Parameter Name | Value |
|---|---|
| Path Number Parameter $L$ | 10 |
| Fading Parameter $a_0$ | 8.21 |
| Fading Parameter $a_1$ | 12.37 |
| Fading Parameter $a_2$ | 0.02 |
| Impulsive Noise Power | -15dB |
| Impulsive Index $A$ | 0.1 |
| Gauss Noise Power | 2.5dB |

## V. SIMULATION RESULTS

In this section, we show numerical results of the performance for HWPLC relaying systems. We use MATLAB to build simulations to compare numerical results with those found from the analytical model developed in this paper. The simulation parameters are chosen based on the HomePlug AV2 standard [30], configured as Table I. In addition, we set the parameter $p$ in (25) as $3.27 \times 10^{-3}$ according to [12]. We consider two cases with the fixed values of the SNR $\gamma_p, \gamma_w$, i.e., 5, 30.

According to [28], values of parameters $\omega_i$ and $q_i$ are tabulated in Table II. In addition, to simulate the wireless channel with fading Nakagami-$m$, we set the parameters $m$ and $\Omega$ in (15), respectively, as two and one. As in (33), (43), and (53), the accuracy of the numerical results depend on $N$, i.e., a large $N$ leads to a more accurate approximation. In our numerical results, we set $N = 10$.

Fig. 4 demonstrates the average channel capacity $C_{av}$ versus $\gamma$ of the HWPLC relaying system. The numerical results are obtained by (33). Note that the closed-form in (33) is an approximation of the real value of $C_{av}$. From Fig. 4, we observe that the numerical results are almost consistent with the analytical expression. A small performance gap is due to the limited value of $N$. Also, the capacity increases linearly with the SNR $\gamma$. This can be verified by (33), where $C_{av}$ is a linear function of $\ln \gamma_w$ (or $\ln \gamma_p$). Furthermore, approximation is more accurate in high SNR region.

By comparing Fig. 4(a) and (b), we can notice that the transmit SNRs of the PLC and wireless channels have similar influence on the system capacity which can also be verified by (33). In addition, when one involved channel is out of work (or works with a very low SNR, such as 5 dB), the HWPLC relaying system still can work effectively with high capacity if the other channel has a high SNR. In Fig. 4, $\gamma_p = 0$ and $\gamma_w = 0$ represent the cases of wireless-only and PLC-only transmissions, respectively. We can observe when introducing a PLC channel to cooperate with the wireless channel, the capacity of the system increases with the $\gamma_p$ due to the parallel

$$\begin{aligned} B_{av} = 2 \min &\left( \sum_{j=0}^{1} \sum_{i=1}^{N} w_i \frac{p_j}{\sqrt{\pi}} \Phi\left(a_0 - a_1 \left(\frac{2q_i^2}{\alpha_j \gamma_p}\right)^{-a_2/\lambda}\right), \frac{a}{\sqrt{\pi}\Gamma(m)} \sum_{i=1}^{N} w_i \Upsilon\left(m, \frac{2mq_i^2}{b\gamma_w \Omega}\right) \right) \\ &- \left( \min \left( \sum_{j=0}^{1} \sum_{i=1}^{N} w_i \frac{p_j}{\sqrt{\pi}} \Phi\left(a_0 - a_1 \left(\frac{2q_i^2}{\alpha_j \gamma_p}\right)^{-a_2/\lambda}\right), \frac{a}{\sqrt{\pi}\Gamma(m)} \sum_{i=1}^{N} w_i \Upsilon\left(m, \frac{2mq_i^2}{b\gamma_w \Omega}\right) \right) \right)^2 \end{aligned} \tag{53}$$

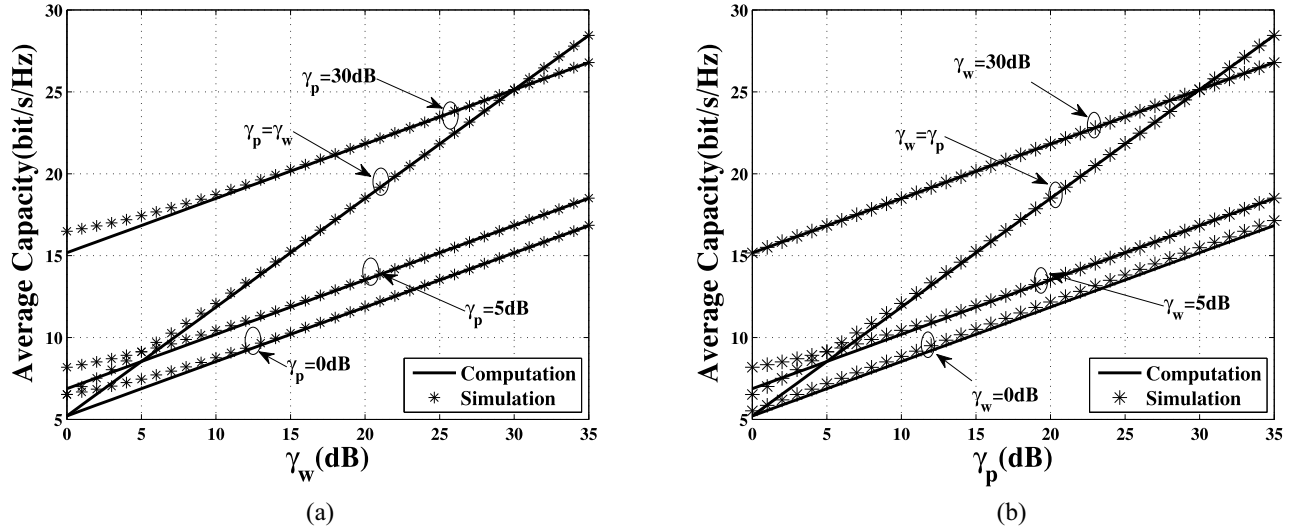


Fig. 4. Comparison of the average capacity between Monte-Carlo simulation and our computation with different SNRs. (a) Capacity against $\gamma_w$ with various $\gamma_p$. (b) Capacity against $\gamma_p$ with various $\gamma_w$.

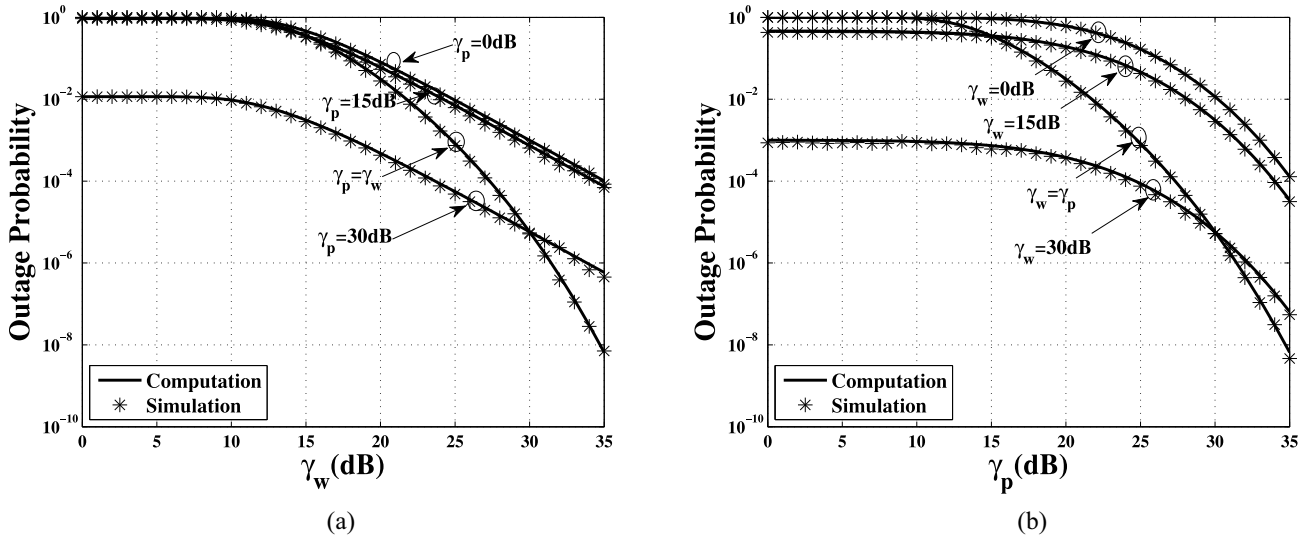


Fig. 5. Comparison of the outage probability between Monte-Carlo simulation and our computation with different SNRs. (a) Outage probability against $\gamma_w$ with various $\gamma_p$. (b) Outage probability against $\gamma_p$ with various $\gamma_w$.

TABLE II
VALUES OF SIMULATION PARAMETERS $\omega_i$, $q_i$

| $i$ | 1 | 2 | 3 | 4 | 5 | 6 | 7 | 8 | 9 | 10 |
|---|---|---|---|---|---|---|---|---|---|---|
| $\omega_i$ | 4.622E-1 | 2.866E-1 | 1.090E-1 | 2.481E-2 | 3.243E-3 | 2.283E-4 | 7.803E-6 | 1.086E-7 | 4.399E-10 | 2.229E-13 |
| $q_i$ | $\pm 0.24$ | $\pm 0.73$ | $\pm 1.23$ | $\pm 1.73$ | $\pm 2.25$ | $\pm 2.78$ | $\pm 3.34$ | $\pm 3.94$ | $\pm 4.60$ | $\pm 5.38$ |

transmissions in the two channels. The similar results can also be obtained when we add a wireless channel to the PLC-only systems.

Fig. 5 shows the curves of the outage probability with the transmission rate $R = 10$ bit/s/Hz versus the transmit SNR. The analytical results are obtained by using the closed-form expression given by (43). In two subfigures, the analytical results and the simulation results are consistent. Moreover, the outage performance is obviously improved with increasing transmit SNRs $\gamma_p$ and $\gamma_w$.

From Fig. 5(a), it is observed that the outage probability is high when $\gamma_w$ is lower than 10 dB and $\gamma_p$ is 5 dB. However, when the $\gamma_w$ is larger than 10 dB, the outage rate decreased dramatically. The reason is when $\gamma_p$ is 5 dB, when $\gamma_w \geq$ 5 dB, wireless interface has been selected. In Fig. 5(b), when the $\gamma_p$ is larger than 22 dB and the $\gamma_w$ is set as 5 dB, the outage probability of the system decreases for the reason that when $\gamma_p \geq 22$ dB and $\gamma_w = 5$ dB, the wireless channel is no longer selected to forward information and the PLC channel with a higher SNR is specified. When adding a PLC channel

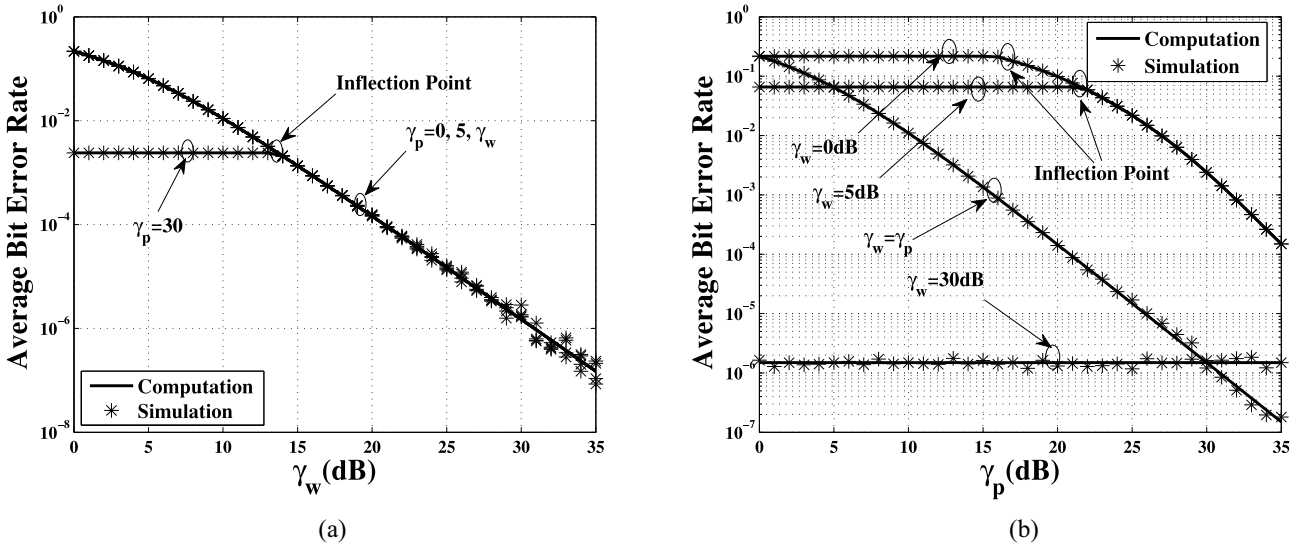


Fig. 6. Comparison of the average BER between Monte-Carlo simulation and our computation with different SNRs. (a) Average BER against $\gamma_w$ with various $\gamma_p$. (b) Average BER against $\gamma_p$ with various $\gamma_w$.

with the transmit SNR lower than 15 dB to cooperate with the wireless-only channel, the average outage probability does not obviously change. However, when a PLC channel with $\gamma_p \geq 30$ dB is used to cooperate with the wireless channel, the outage probability decreases dramatically. The reason is that the outage probability of a hybrid channel is decided by the channel with lower outage and the PLC channel with transmit SNR 30 dB has a very low outage probability.

Fig. 6 demonstrates the plots of the average BER versus the transmit SNR. The analytical curves obtained from (53) are consistent with the simulation curves which validates the correctness of the derivation. As the increasing of $\gamma_w$, the BER performance of the HWPLC relaying system is significantly improved.

In Fig. 6(a), when $\gamma_p$ is set as 5 dB, the BER is dominated by the $\gamma_w$ because the wireless channel is selected as the communication channel due to its higher received SNR. However, when $\gamma_p = 30$ dB, there exist two distinct regions in the curves of BER. When the quality of the wireless channel is poor ($\gamma_w \leq 13$ dB), BER is dominated by the BER of the PLC channel given in (53).

There also exists an infection point when $\gamma_w$ is set as 5 dB or 0 dB in Fig. 6(b), which can be verified by (53). The infection point means that the BER plot is dominated by BER of the wireless channel. From the plot $\gamma_w = 5$ dB, BER does not change until $\gamma_p$ is around or lager than 21 dB, since when $\gamma_p \geq 21$ the PLC channel is selected to forward messages. However, if we set $\gamma_w$ as 30 dB, BER keeps almost unchanged as about $10E{-}5.8$, which is not influenced by the increasing of the $\gamma_p$. Hence, it illustrates that the HWPLC relaying channel can adaptively choose the channel with lower BER to transmit message. Interestingly, if we set $\gamma_w = 0$ dB, SER does not change as $\gamma_p \leq 21$ dB. By comparing with Fig. 5(b), we find that the outage probability of the hybrid channel leads to a high SER. In addition, SER of the HWPLC channel is lower than that of the wireless-only channel when the PLC channel of the HWPLC channel has high transmit SNR. More obviously, BER performance of the HWPLC channel is much better than that of PLC-only channel.

## VI. Conclusion

In this paper, we analyze an HWPLC relaying system that improves the capacity and reliability for IoT networks. Both wireless and PLC interface are installed at the relaying node. For the dual-interface relay, the interface with a higher received SNR is selected as the information forwarder at the relay. The optimal SNR for the diversity PLC channel is obtained with MRC. Accordingly, we derive the CDF of the received SNRs of the PLC and the wireless channel with Nakagami-*m* fading. Capitalizing on the extracted CDF formula of the SNR at the destination, novel closed-form expressions for the average channel capacity, outage probability, and BER are obtained. Simulation results verify the accuracy and the correctness of the proposed analyses. Furthermore, simulation results show that the system performances are dramatically improved when adopting hybrid PLC and wireless communication interface at the relay.

## References

[1] Z. Khan *et al.*, "IoT connectivity in radar bands: A shared access model based on spectrum measurements," *IEEE J. Sel. Areas Commun.*, vol. 55, no. 2, pp. 88–96, Feb. 2017.

[2] Y.-W. Qian *et al.*, "Performance analysis for a two-way relaying power line network with analog network coding," *Front. Inf. Technol. Electron. Eng.*, vol. 16, no. 10, pp. 892–898, 2015.

[3] T. R. Oliveira, C. A. G. Marques, M. S. Pereira, S. L. Netto, and M. V. Ribeiro, "The characterization of hybrid PLC-wireless channels: A preliminary analysis," in *Proc. IEEE Int. Symp. Power Line Commun. Appl. (ISPLC)*, Johannesburg, South Africa, 2013, pp. 98–102.

[4] S. W. Lai and G. G. Messier, "The wireless/power-line diversity channel," in *Proc. IEEE Int. Conf. Commun. (ICC)*, Cape Town, South Africa, 2010, pp. 1–5.

[5] F. Salvadori, C. S. Gehrke, A. C. de Oliveira, M. de Campos, and P. S. Sausen, "Smart grid infrastructure using a hybrid network architecture," *IEEE Trans. Smart Grid*, vol. 4, no. 3, pp. 1630–1639, Sep. 2013.

[6] L. M. L. Oliveira, J. Reis, J. J. P. C. Rodrigues, and A. F. de Sousa, "IOT based solution for home power energy monitoring and actuating," in *Proc. IEEE Int. Conf. Ind. Informat. (INDIN)*, Cambridge, U.K., 2015, pp. 988–992.

[7] A. Mckeown, H. Rashvand, T. Wilcox, and P. Thomas, "Priority SDN controlled integrated wireless and powerline wired for smart-home Internet of Things," in *Proc. UIC-ATC-ScalCom*, Beijing, China, 2015, pp. 1825–1830.

[8] Y. Chen, J. K. Hwang, and S. M. Wu, "A reliable power line carrier and wireless data concentrator for broadband energy information network," *IEEE Trans. Consum. Electron.*, vol. 49, no. 4, pp. 1054–1060, Nov. 2003.

[9] A. Mengi *et al.*, "IEEE 1905.1 hybrid home networking standard and its implementation with PLC, Wi-Fi and Ethernet technologies," in *Proc. Int. Symp. Power Line Commun. Appl. (ISPLC)*, Bottrop, Germany, 2016, pp. 162–166.

[10] *IEEE Standard for a Convergent Digital Home Network for Heterogeneous Technologies*, IEEE Standard 1905.1, 2013.

[11] N. Kushiro, T. Higuma, M. Nakata, H. Kubota, and K. Sato, "Practical solution for constructing ubiquitous network in building and home control system," *IEEE Trans. Consum. Electron.*, vol. 53, no. 4, pp. 1387–1392, Nov. 2007.

[12] A. Dubey, R. K. Mallik, and R. Schober, "Performance analysis of a power line communication system employing selection combining in correlated log-normal channels and impulsive noise," *IET Commun.*, vol. 8, no. 7, pp. 1072–1082, May 2014.

[13] H. Zou, A. Chowdhery, S. Jagannathan, J. M. Cioffi, and J. LeMasson, "Multi-user joint subchannel and power resource-allocation for power-line relay networks," in *Proc. IEEE Int. Conf. Commun. (ICC)*, Dresden, Germany, 2009, pp. 1–5.

[14] P. Popovski and H. Yomo, "Physical network coding in two–way wireless relay channels," in *Proc. IEEE Int. Conf. Commun. (ICC)*, Glasgow, U.K., 2007, pp. 707–712.

[15] S. Galli, A. Scaglione, and Z. Wang, "For the grid and through the grid: The role of power line communications in the smart grid," *Proc. IEEE*, vol. 99, no. 6, pp. 998–1027, Jun. 2011.

[16] M. Sebeck and G. Bumiller, "A network management system for power-line communications and its verification by simulation," in *Proc. IEEE Int. Conf. Power Line Commun. Appl. (ISPLC)*, 2000, pp. 225–232.

[17] L. Lampe, R. Schober, and S. Yiu, "Distributed space-time coding for multihop transmission in power line communication networks," *IEEE J. Sel. Areas Commun.*, vol. 24, no. 7, pp. 1389–1400, Jul. 2007.

[18] L. Lampe and A. J. H. Vinck, "On cooperative coding for narrow band PLC networks," *AEU Int. J. Electron. Commun.*, vol. 65, no. 8, pp. 681–687, 2011. [Online]. Available: http://www.vadosezonejournal.org

[19] T.-E. Sung and A. Bojanczyk, "Optimal power control and relay capacity for PLC-embedded cooperative systems," in *Proc. IEEE Consum. Commun. Netw. Conf. (CCNC)*, Las Vegas, NV, USA, 2010, pp. 1–5.

[20] M. Kuhn, S. Berger, I. Hammerstrom, and A. Wittneben, "Power line enhanced cooperative wireless communications," *IEEE J. Sel. Areas Commun.*, vol. 24, no. 7, pp. 1401–1410, Jul. 2010.

[21] G. Bumiller, L. Lampe, and H. Hrasnica, "Power line communication networks for large-scale control and automation systems," *IEEE Commun. Mag.*, vol. 48, no. 4, pp. 106–113, Apr. 2010.

[22] D. G. Brennan, "Linear diversity combining techniques," *Proc. IEEE*, vol. 91, no. 2, pp. 331–356, Feb. 2003.

[23] N. C. Beaulieu and F. Rajwan, "Highly accurate simple closed-form approximations to lognormal sum distributions and densities," *IEEE Commun. Lett.*, vol. 8, no. 12, pp. 709–712, Dec. 2004.

[24] I. S. Gradshteyn and I. Ryzhik, *Table of Integrals, Series, and Products*, 7th ed. Amsterdam, The Netherlands: Elsevier, 2007.

[25] K. C. Wiklundh, P. F. Stenumgaard, and H. M. Tullberg, "Channel capacity of Middleton's class a interference channel," *Electron. Lett.*, vol. 45, no. 24, pp. 1227–1229, Nov. 2009.

[26] M. Sheikh-Hosseini, G. A. Hodtani, and M. Molavi-Kakhki, "Capacity analysis of power line communication point-to-point and relay channels," *Trans. Emerg. Telecommun. Technol.*, vol. 27, no. 2, pp. 200–215, 2016.

[27] A. Dubey and R. K. Mallik, "Effect of channel correlation on multi-hop data transmission over power lines with decode-and-forward relays," *IET Commun.*, vol. 10, no. 13, pp. 1623–1630, Sep. 2016.

[28] M. Abramowitz and I. A. Stegun, *Handbook of Mathematical Functions With Formulas, Graphs, and Mathematical Tables*, 9th ed. New York, NY, USA: Dover, 1970.

[29] M. R. McKay, A. J. Grant, and I. B. Collings, "Performance analysis of MIMO-MRC in double-correlated Rayleigh environments," *IEEE Trans. Commun.*, vol. 55, no. 3, pp. 497–507, Mar. 2007.

[30] Powerline-Alliance, "Homeplug AV white paper," HomePlug Powerline Alliance Inc., San Ramon, CA, USA, Tech. Rep. HPAVWP-050818, 2005.

**Yuwen Qian** received the Ph.D. degree in automatic engineering from the Nanjing University of Science and Technology, Nanjing, China, in 2011.

From 2002 to 2011, he was a Lecturer with the Automation School, Nanjing University of Science and Technology, where he has been a Lecturer with the School of Electronic and Optical Engineering since 2011. His current research interests include information security, smart grids, and power line communications.

**Jiahui Yan** received the B.E. degree in electronic information engineering from Nanjing Normal University, Nanjing, China, in 2015. She is currently pursuing the M.E. degree in communication and information system at the Nanjing University of Science and Technology, Nanjing.

Her current research interests include opportunistic relaying networks in PLC and hybrid networks of PLC and wireless.

**Haibing Guan** received the Ph.D. degree from Tongji University, Shanghai, China, in 1999.

He is currently a Professor with the School of Electronic, Information and Electronic Engineering, Shanghai Jiao Tong University, Shanghai, and the Director of the Shanghai Key Laboratory of Scalable Computing and Systems. His current research interests include distributed computing, network security, network storage, green IT, and cloud computing.

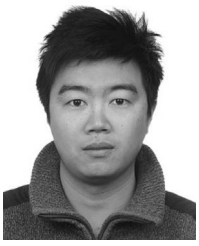

**Jun Li** (M'09–SM'16) received the Ph.D. degree in electronic engineering from Shanghai Jiao Tong University, Shanghai, China, in 2009.

In 2009, he was with the Department of Research and Innovation, Alcatel Lucent Shanghai Bell, Beijing, China, as a Research Scientist for five months. From 2009 to 2012, he was a Post-Doctoral Fellow with the School of Electrical Engineering and Telecommunications, University of New South Wales, Sydney, NSW, Australia. From 2012 to 2015, he was a Research Fellow with the School of Electrical Engineering, University of Sydney, Sydney. Since 2015, he has been a Professor with the School of Electronic and Optical Engineering, Nanjing University of Science and Technology, Nanjing, China. His current research interests include network information theory, channel coding theory, wireless network coding, and resource allocations in cellular networks.

**Xiangwei Zhou** (GS'08–M'13–SM'17) received the bachelor's degree in communication engineering from the Nanjing University of Science and Technology, Nanjing, China, in 2005, the master's degree in information and communication engineering from Zhejiang University, Hangzhou, China, in 2007, and the Ph.D. degree in electrical and computer engineering from the Georgia Institute of Technology, Atlanta, GA, USA, in 2011.

Since 2015, he has been an Assistant Professor with the Division of Electrical and Computer Engineering, Louisiana State University, Baton Rouge, LA, USA. He was an Assistant Professor with the Department of Electrical and Computer Engineering, Southern Illinois University, Carbondale, IL, USA, from 2013 to 2015, and a Senior Systems Engineer with Marvell Semiconductor, Santa Clara, CA, USA, from 2011 to 2013. His current research interests include wireless communications, statistical signal processing, and cross-layer optimization, with current emphasis on spectrum and energy efficient communications, coexistence of wireless systems, and machine learning for intelligent communications.

Dr. Zhou was a recipient of the Best Paper Award of the 2014 International Conference on Wireless Communications and Signal Processing.

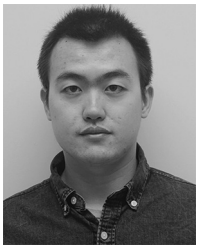

**Shengjie Guo** received the B.Eng. degree from the University of Electronic Science and Technology of China, Chengdu, China, in 2012. He is currently pursuing the Ph.D. degree at Louisiana State University, Baton Rouge, LA, USA.

His current research interests include energy efficiency in wireless communications, D2D communications, Internet of Things, and energy harvesting in communications networks.

**Dushantha Nalin K. Jayakody** (M'14) received the B.Eng. (First Class Hons.) degree in 2009 and was ranked as the merit position holder of the University (under SAARC Scholarship), the M.Sc. degree in electronics and communications engineering from the Department of Electrical and Electronics Engineering, Eastern Mediterranean University, Famagusta, Cyprus, in 2010 (under the University full graduate scholarship) and ranked as the first merit position holder of the department, and the Ph.D. degree in electronics and communications engineering from the University College Dublin, Dublin, Ireland, in 2014.

From 2014 to 2016, he was a Post-Doctoral Fellow with the Coding and Information Transmission Group, University of Tartu, Tartu, Estonia, and the University of Bergen, Bergen, Norway. Since 2016, he has been a Professor with the Department of Control System Optimization, Institute of Cybernetics, National Research Tomsk Polytechnic University, Tomsk, Russia.

Dr. Jayakody has served as the Session Chair or a Technical Program Committee member for various international conferences such as IEEE PIMRC 2013/2014, IEEE WCNC 2014/2016, and IEEE VTC 2015.